



Since January 2020 Elsevier has created a COVID-19 resource centre with free information in English and Mandarin on the novel coronavirus COVID-19. The COVID-19 resource centre is hosted on Elsevier Connect, the company's public news and information website.

Elsevier hereby grants permission to make all its COVID-19-related research that is available on the COVID-19 resource centre - including this research content - immediately available in PubMed Central and other publicly funded repositories, such as the WHO COVID database with rights for unrestricted research re-use and analyses in any form or by any means with acknowledgement of the original source. These permissions are granted for free by Elsevier for as long as the COVID-19 resource centre remains active.



# Survey of air exchange rates and evaluation of airborne infection risk of COVID-19 on commuter trains

Naohide Shinohara<sup>a,\*</sup>, Jun Sakaguchi<sup>b</sup>, Hoon Kim<sup>c</sup>, Naoki Kagi<sup>d</sup>, Koichi Tatsu<sup>e</sup>, Hiroyuki Mano<sup>a</sup>, Yuichi Iwasaki<sup>a</sup>, Wataru Naito<sup>a</sup>

<sup>a</sup> National Institute of Advanced Industrial Science and Technology (AIST), 16-1 Onogawa, Tsukuba, Ibaraki 305-8569, Japan

<sup>b</sup> University of Niigata Prefecture, 471 Ebigase, Higashi-ku, Niigata-City, Niigata 950-8680, Japan

<sup>c</sup> National Institute of Public Health, 2-3-6 Minami, Wako, Saitama 351-0197, Japan

<sup>d</sup> Tokyo Institute of Technology, 2-12-1 Ookayama, Meguro-ku, Tokyo 152-8552, Japan

<sup>e</sup> Isuzu Motors Ltd., 8 Tsuchidana, Fujisawa, Kanagawa 252-8501, Japan

## ARTICLE INFO

Handling Editor: Xavier Querol

### Keywords:

SARS-CoV-2  
Droplet nuclei  
Commuter  
Ventilation  
Airflow velocity  
Transmission

## ABSTRACT

To identify potential countermeasures for coronavirus disease (COVID-19), we determined the air exchange rates in stationary and moving train cars under various conditions in July, August, and December 2020 in Japan. When the doors were closed, the air exchange rates in both stationary and moving trains increased with increasing area of window-opening (0.23–0.78/h at 0 m<sup>2</sup>, windows closed to 2.1–10/h at 2.86 m<sup>2</sup>, fully open). The air exchange rates were one order of magnitude higher when doors were open than when closed. With doors closed, the air exchange rates were higher when the centralized air conditioning (AC) and crossflow fan systems (fan) were on than when off. The air exchange rates in moving trains increased as train speed increased, from 10/h at 20 km/h to 42/h at 57 km/h. Air exchange rates did not differ significantly between empty cars and those filled with 230 mannequins representing commuters. The air exchange rates were lower during aboveground operation than during underground. Assuming that 30–300 passengers travel in a train car for 7–60 min and that the community infection rate is 0.0050–0.30%, we estimated that commuters' infection risk on trains was reduced by 91–94% when all 12 windows were opened (to a height of 10 cm) and the AC/fan was on compared with that when windows were closed and the AC/fan was off.

## 1. Introduction

Caused by severe acute respiratory syndrome coronavirus 2 (SARS-CoV-2), coronavirus disease 2019 (COVID-19) was first reported in December 2019 in Wuhan, China (Zhu et al., 2020), and expanded globally during 2020–2021 (WHO, 2020; 2021). One particular concern is the risk of infection in crowded commuter trains (MHLW, 2021). Given that a large proportion of the population in Japan uses public transportation including trains and buses, effective and practical measures to attenuate the risk of COVID-19 infection associated with public transport are urgently required.

SARS-CoV-2-containing droplets are emitted from infected persons through breathing, talking, coughing, and sneezing. Large droplets (mostly larger than a few tens of micrometers in diameter) are deposited rapidly onto the floor within a distance of 2 m from the infected persons, whereas small droplet nuclei (i.e. the residue of dried aerosols that result

from the evaporation of droplets; mostly smaller than several micrometers in diameter) can remain suspended in air for more than 1 h before deposition or air exchange (Wells 1934; Xie et al. 2007). Whereas larger droplets are removed from indoor air predominantly through their deposition on floors and walls, small droplet nuclei are removed primarily thorough air exchange (Yang and Marr, 2011). By definition, droplet transmission is accomplished through the direct deposition of droplets onto mucosae or conjunctiva and their inhalation; airborne transmission is due to the inhalation of droplet nuclei; and contact-based transmission arises after contact with a polluted surface and the transfer of virus to the mucosae or conjunctiva via touching the eyes, nose, and mouth (WHO, 2020; 2021). Bourouiba (2021), who reviewed the fluid dynamics of disease transmission, emphasized the importance of the size and nature of inhaled particles to understand range and evolution of the droplet nuclei and their ability to penetrate deep into the respiratory tract. The biological plausibility of airborne transmission can be rated

\* Corresponding author.

E-mail address: [n-shinohara@aist.go.jp](mailto:n-shinohara@aist.go.jp) (N. Shinohara).

<https://doi.org/10.1016/j.envint.2021.106774>

Received 6 April 2021; Received in revised form 9 July 2021; Accepted 12 July 2021

Available online 23 July 2021

0160-4120/© 2021 The Authors. Published by Elsevier Ltd. This is an open access article under the CC BY license (<http://creativecommons.org/licenses/by/4.0/>).

according to three factors: generation of pathogen containing aerosol, its viability in the environment, and its access to target tissue (Jones and Brosseau, 2015). The biological plausibility of airborne transmission with SARS-CoV-2 has been rated as high because the air surrounding COVID-19 patients contains viable SARS-CoV-2, because SARS-CoV-2 remains viable in aerosol for a certain period of time, and because SARS-CoV-2 can directly reach its receptor, angiotensin-converting enzyme 2 (ACE 2), in the respiratory tract and alveoli (Tang et al., 2020). In particular, although viruses in aerosol generally become inactivated over time, SARS-CoV-2 is persistent for a certain period of time (median viability, 1.1 h; 95% confidence interval, 0.6–2.6 h) (van Doremalen et al. 2020).

Virus transmission from large droplets (droplet transmission) can be prevented through the appropriate use of face masks, protective shields, and social distancing. Ventilation is a critical countermeasure to transmission through droplet nuclei (airborne transmission). Numerous studies have measured air exchange rates in buildings as a first step towards decreasing the exposure to volatile chemicals and particulate matter in indoor air (Beko et al. 2010; Shinohara et al. 2011; 2013). Although computational fluid dynamics (CFD) calculations are used to estimate air exchange rates and the diffusion of droplet nuclei (Asai, 1995; Wang et al., 2014; Li et al. 2019), these factors have not been surveyed on commuter trains.

Many studies have indicated possible airborne transmission of COVID-19 (Tang et al., 2020) in various environments, such as on a bus (Shen et al., 2020) and in a restaurant (Li et al., 2021). Dose-response model and Wells–Riley model have both been used to estimate the airborne infection risk (To and Chao, 2010). A dose-response model is based on the amount of exposure to the virus, obtained through measurements or simulations, and a dose-response curve, obtained from an epidemiological study or animal test. The dose-response model can be applied simultaneously to multiple exposure pathways (Haas, 1983; Nicas and Sun, 2006; Nicas and Jones, 2009; Haas et al., 2014), and the model have used to estimate the risk of COVID-19 for healthcare workers (Mizukoshi et al., 2021) and for individual participants of mass-

gatherings (Murakami et al., 2021). The Wells–Riley model, which is specific to estimating airborne infection risk, is based on quanta generation rates, which are collected from epidemical studies, and dilution factors (air exchange rates and deposition rates), which are obtained through measurements or simulations (Riley et al., 1978). Quanta generation rates (Buonanno et al., 2020; Dai and Zhao, 2020; Miller et al., 2020) and airborne infection risks (Harrichandra et al., 2020; Schijven et al., 2020) for COVID-19 have been evaluated. The basic reproductive number ( $R_0$ ) for COVID-19 can be decreased by reducing the commute time and number of passengers on buses (Chen et al., 2021). However, no previous study has evaluated the risk reduction for COVID-19 associated with improved ventilation and window-opening in vehicles.

Here, we determined the air exchange rates on commuter train cars in Japan under several conditions, to understand the effects of potential countermeasures against COVID-19. Then, we estimated the airborne infection risk of COVID-19 by using a dose-response model with the measured air exchange rates and assumed community infection rates, commute time, and number of passengers.

## 2. Materials and methods

### 2.1. Survey period and trains

During 3 periods in 2020 (17–19 July, 14–16 August, and 11–13 December), we determined the air exchange rates in a commuter train (Tokyo Metro Series 16000). Each train comprised 10 cars; each car had a total volume of 107.1 m<sup>3</sup> and had seats for 54 passengers, 12 windows that could be opened, and 8 doors. Four air intakes for the air conditioner (AC) are placed on both sides of the ceiling over benches, and outlet along each side of ceiling (Fig. 1). Crossflow fans are placed at the center of ceiling (Fig. 1) blow air downwards and towards the wall. A ventilation system is not installed because it requires frequent maintenance owing to the particles in air in the underground tunnel.

Of the 10 cars, we used the 3rd and 8th cars for measuring air exchange rate because these cars do not have underfloor equipment that

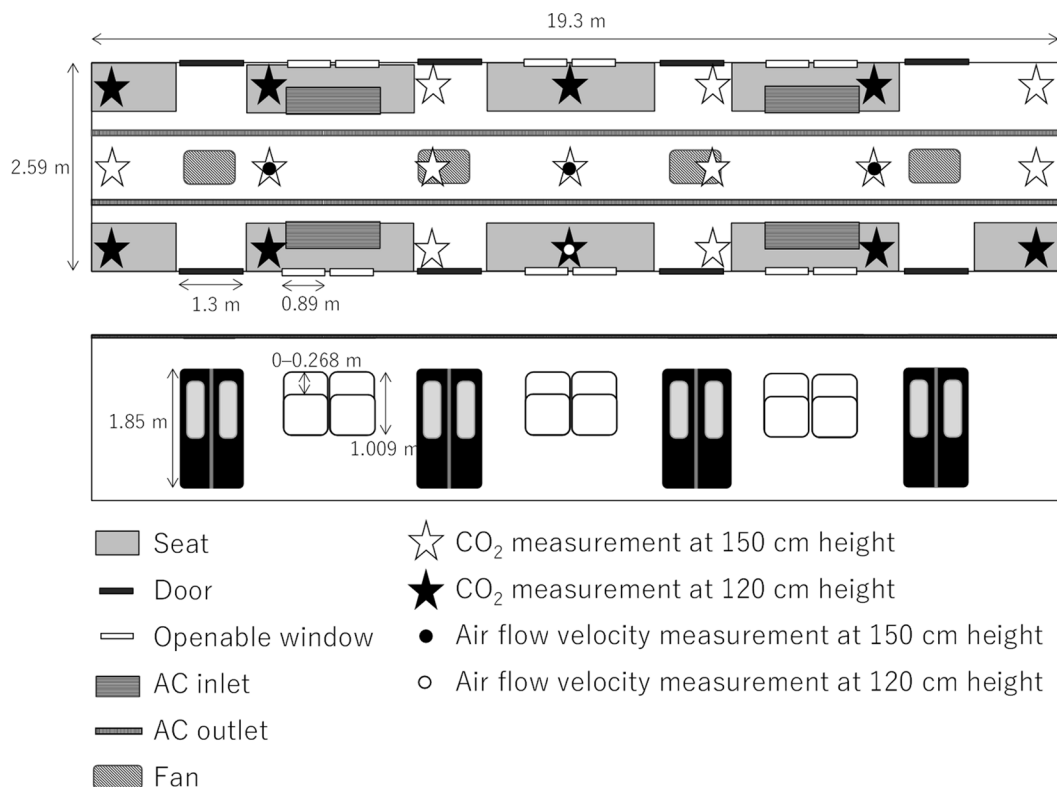


Fig. 1. Schematic diagram of the sampling sites in the train cars.

generates heat, such as a motor. Stationary tests were conducted at Ayase Depot (Adachi, Tokyo, Japan). Moving tests were conducted aboveground between Ayase- and Kitasenju- stations (2.5 km) and underground between Kitasenju- and Kasumigaseki- stations (12 km). Air flow velocity was measured in the 3rd car, and airtightness was measured in the 5th car.

## 2.2. Determination of air exchange rates

The air exchange rates were measured by using the CO<sub>2</sub> decay method (JISC, 1984; ASTM, 1998), which is appropriate for determining short-term air exchange rates in unoccupied rail cars. In brief, CO<sub>2</sub> was emitted from gas cylinders into the cars. Indoor air was agitated by using circulators (EAC-23-W, Iris Ohyama Inc., Sendai, Japan) and blowers (Earthman BW-144LiAX, Takagi Co., Ltd., Kitakyushu, Japan) until the CO<sub>2</sub> concentrations reached equilibrium across all 21 sampling points in the cars. Then, the indoor CO<sub>2</sub> concentration was monitored every 10 s at all sampling points in each car (Fig. 1) at heights of 1.5 m (representing standing passengers) and 1.2 m (0.7 m from the seat surface; representing seated passengers) for 15 min to 2 h with a CO<sub>2</sub> monitor (MCH-383SD, Lutron Electronic Enterprise Co., Taipei, Taiwan, or TR-76Ui, T & D Co., Matsumoto, Japan). The outdoor CO<sub>2</sub> concentration was measured before and after each in-car CO<sub>2</sub> measurement. Before each period of the survey (July, August, and December), the CO<sub>2</sub> monitors were calibrated against several concentrations of CO<sub>2</sub> gas, including ambient level, according to a calibrated CO<sub>2</sub> monitor (Model 2211, Kanomax Japan, Inc., Osaka, Japan).

The air exchange rates were obtained by fitting exponential functions to the differences of CO<sub>2</sub> concentrations between inside and outside of the cars.

## 2.3. Stationary tests

Stationary tests were conducted in a closed train depot with negligible wind. In the stationary tests, air exchange rates were evaluated with windows open to different degrees, doors open or closed, centralized air conditioning (AC) and crossflow fan systems (AC/fan) on or off, and passengers (modeled with mannequins) present or not. The tested heights of window opening were 0, 5, 10, 15, and 26.8 cm. Window-opening positions included 2 diagonal points (front right and rear left windows), 6 points on the right and left in the rotational direction, or every 12 points (Fig. S1). For each door-open test, all 4 doors on the same side of the car were opened. The AC and crossflow fan systems were switched on and off together. During August test sessions, 230 fiber-reinforced plastic mannequins without heat sources (143 standing women, 0.0484 m<sup>3</sup>; 37 standing men, 0.0612 m<sup>3</sup>; 47 sitting women, 0.0467 m<sup>3</sup>; 3 sitting men, 0.0612 m<sup>3</sup>; Taiyo Kogei Co., Ltd., Osaka, Japan) were loaded into the car to model crowded conditions. Differences between the temperatures inside cars and outside with all doors closed were 0.35 ± 1.3 °C in July, −12 ± 1.5 °C in August, and 5.0 ± 1.4 °C in December with the AC/fan on, and 1.1 ± 0.83 °C, −9.1 ± 1.2 °C, and 6.4 ± 0.41 °C, respectively, with the AC/fan off.

## 2.4. Moving test

In August 2020, air exchange rates were evaluated during continuous operation at 20, 30, 39, and 57 km/h underground and 52–55 km/h aboveground. To model crowded conditions, 230 mannequins (Taiyo Kogei Co., Ltd.) were loaded into the 8th car. To model empty conditions, the 3rd car was unoccupied. Tests were conducted during the middle of the night, outside of normal business hours. Indoor and outdoor temperatures were 23 ± 0.69 °C and 31 ± 0.44 °C, respectively, aboveground and 23 ± 0.80 °C and 31 ± 0.21 °C underground. The average wind speed in Tokyo during the moving test hours at the date was 1.8 m/s (JMA, 2021).

## 2.5. Air flow velocity and airtightness

During August 2020, air flow velocity (10-s average) in the 3rd car was measured at 4 points every 10 s with a multi-channel thermal anemometer with a platinum wire (Anemomaster Model 1560 and Omni-directional Probe Model 0965-01, Kanomax Japan Inc.). Three sampling points were located along the center of the aisle at a height of 1.5 m, with the remaining point above a seat at a height of 1.2 m (Fig. 1). The total leakage area of the train was measured with an airtightness measurement instrument (Dr. Dolphin OMAT2000, EOM Co., Shizuoka, Japan). To assess the airtightness of the cars, the equivalent leakage area per floor area (C-value) was calculated by dividing the total area of any gaps by the total floor area, which included the seating surface.

## 2.6. Evaluation of airborne infection risk

We estimated the airborne infection risk of COVID-19 for passengers on commuter trains that was attributable to inhalation of droplet nuclei under several conditions by varying community infection rate, number of passengers on the train, commute time, AC/fan on or off, and exposure to infected persons who were talking or silent. We did not estimate droplet transmission due to direct deposition on mucosae or conjunctiva or to inhalation of large droplets, because almost all commuters in Japan have worn masks, which exclude large droplets, since winter 2020; therefore, the occurrence of droplet transmission on commuter trains in Japan was minimal. In addition, we did not estimate contact-base transmission, because viral copies of SARS-CoV-2 were not detected at high concentrations on surfaces even in rooms inhabited by infected persons (Yamagishi et al. 2020).

Community infection rates, defined as the proportion of infected persons in a target population at a specific time, varied between 0.0050% and 0.30%, indicating that 50–3000 people become infected daily during 14 consecutive days in Tokyo, which has 14 million inhabitants (Tokyo Metropolitan Government, 2019) referencing the maximum daily new positive cases of COVID-19 infection in Tokyo (2520 persons (January 7, 2021); Tokyo Metropolitan Government, 2021). The number of passengers in a train car varied between 2 and 300 referencing the congestion rates during morning commuting hour in Tokyo metropolitan area in 2019 (average, 163%; maximum, 199%; MLIT, 2020) and capacity of the train car used in this study (151 persons), and commute time varied between 1 and 60 min referencing the total travel times between the termini for 9 lines of Tokyo Metro (35–51 min; Tokyo Metro, 2021).

The concentration of virus to which a passenger in commuter train was exposed was estimated by using two-zone (i.e., near-field and far-field) model (Spencer and Plisko, 2007). We assumed that passengers in both the near-field and far-field of an infected person were exposed to virus contained in droplet nuclei that originated from that person (Fig. S2). Although some passengers could expose to droplet nuclei exhaled from multiple infectors when multiple infectors ride on the train car, we assumed that near-fields did not overlap with each other to simplify the calculation. The two-zone model (Spencer and Plisko, 2007) was expressed as:

Near-field:

$$\frac{dC_{near-m}(t)}{dt} = \frac{E}{V_{near}} + \frac{F}{V_{near}}C_{far-m}(t) - \frac{F}{V_{near}}C_{near-m}(t) - \frac{Id_{inhalation}n_{near}C_{near-m}(t)}{V_{near}} - (\lambda + d)C_{near-m}(t) \quad (1)$$

Far-field:

$$\frac{dC_{far-m}(t)}{dt} = \frac{F}{V_{far-m}}C_{near-m}(t)m - \frac{F}{V_{far-m}}C_{far-m}(t)m - \frac{Id_{inhalation}n_{far-m}C_{far-m}(t)}{V_{far-m}} - (\lambda + N + d)C_{far-m}(t) \quad (2)$$

**Table 1**

Parameters and parameter derivation methods used to calculate risk.

Symbols	Unit	Description		Value	Derivation	Reference
$k$	/PFU	dose–response function for SARS-CoV-2		0.00246	survival probability for SARS-CoV	Watanabe et al., 2010; Mitchell and Weir, 2020; Mizukoshi et al., 2021
$C(t)$	PFU/m <sup>3</sup>	estimated exposure concentrations to the virus		–	$C_{near}(t)$ or $C_{far}(t)$	–
$I$	m <sup>3</sup> /h	inhalation rate or exhalation rate	Silent	0.37	inhalation rate during rest	AIST, 2007
			Talking	0.60	inhalation rate during light-work	AIST, 2007
$r$	–	community infection rate		0.0050–0.30%	Daily infected person are 50–3,000 persons/day for 14 days in Tokyo prefecture (population of Tokyo: 1.4 million)	–
$n$	person	commuter numbers in the train.		2–300	The congestion rates during morning commuting hour in Tokyo metropolitan area in 2019 was averaged 163%. The capacity of the train car used in this study was 151 persons	MLIT, 2020
$t$	min	commuting time		2–60	The total travel times between the termini of Tokyo Metro were 35–51 min	Tokyo Metro, 2021
$C_{near}(t)$	PFU/m <sup>3</sup>	concentration of virus in near-field in train car		–	Equation (1)	–
$C_{far}(t)$	PFU/m <sup>3</sup>	concentration of virus in far-field in train car		–	Equation (2)	–
$E$	PFU/h	emission rates of virus from the infector	Silent	0.0034	$E = C_{copies}/Ratio \times M_D \times I \times e$ (6)	–
			30 s talk per 1 min	0.021		–
$F$	m <sup>3</sup> /h	air flow volume rate from near-field to far-field	AC/fan on	625	half of surface area of near-field $\times$ air flow velocity (0.2 m/s during AC/fan on and 0.01 m/s during AC/fan off)	–
			AC/fan off	31		–
$d_{inhalation}$	–	deposition fractions on alveoli and upper/lower airway		0.5152	deposition fractions on alveolar region (0.2051), conducting airway (0.0822), and head airway (0.228) for 2 $\mu$ m particles (1.005 g/cm <sup>3</sup> of density) calculated using MPPD model (v.3.04)	RIVM, 2017
$\lambda$	/h	inactivation rate		0.66	inactivation rate	van Doremalen et al., 2020
$N$	/h	air exchange rate	window open (10 cm $\times$ 12 points)	27	weighted average of underground air exchange rates for 2 min moving (29, 6.8/h), 20 s stationary (door open) (3.3, 0.59/h), and 10 s stationary (door closed) (30, 30/h)	present study
			window closed	9.5		
$d$	/h	deposition rate on indoor surface		0.35	(underground air exchange rate are assumed to be twice of the aboveground air exchange rate in moving train) deposition on textile	Nicas and Jones, 2009
$V$	m <sup>3</sup>	total indoor volume of the train car		107.1		–
$V_{near}$	m <sup>3</sup>	assumed volume of near-field in train car		0.065	half of oval sphere (minor radius 0.25 m; long radius 0.5 m)	–
$V_{far,m}$	m <sup>3</sup>	assumed volume of far-field in train car		–	Equation (3)	–
$Ratio$	copies/PFU	ratio of virus RNA copies to PFU		1000		Uhteg et al., 2020; Munster et al., 2020
$C_{copies}$	copies/mL	virus RNA copies in saliva		$4 \times 10^6$	median: $3.3 \times 10^6$ copies/mL average: approximately $2 \times 10^6$ copies/mL average: $7 \times 10^6$ copies/mL median: 1 week $10^{6.7}$ copies/mL; 3 weeks $10^{4.9}$	To et al., 2020a Wyllie et al., 2020 Wölfel et al., 2020 To et al., 2020b
$M_D$	mL/m <sup>3</sup>	saliva amount of original droplet of droplet nuclei in the breath air (silent)		$4.6 \times 10^{-6}$	$M_D = M_{DN}/S^3$ (7)	
		saliva amount of original droplet of droplet nuclei in the breath air (10 s talking)		$2.2 \times 10^{-5}$		
$S$	–	ratio of dried droplet nuclei and droplet		0.4	approximately 40% of droplet under < 50 %RH	Yang and Marr, 2011
$M_{DN}$	mL/m <sup>3</sup>	volume of droplet nuclei in the breath air (silent)		$2.9 \times 10^{-7}$	size of dried droplet nuclei: 0.8 $\mu$ m 0.084/cm <sup>3</sup> ; 1.8 $\mu$ m 0.009/cm <sup>3</sup> ; 3.5 $\mu$ m 0.003/cm <sup>3</sup> ; 5.5 $\mu$ m 0.002/cm <sup>3</sup>	Morawska et al., 2009
		volume of droplet nuclei in the breath air (10 s talking)		$1.4 \times 10^{-6}$	size of dried droplet nuclei: 0.8 $\mu$ m 0.236/cm <sup>3</sup> ; 1.8 $\mu$ m 0.068/cm <sup>3</sup> ; 3.5 $\mu$ m 0.007/cm <sup>3</sup> ; 5.5 $\mu$ m 0.011/cm <sup>3</sup>	Morawska et al., 2009
$e$	–	elimination factor of mask		0.5	Average particle removal rate by various types of masks (urethane and non-woven masks)	Tsubokura, 2021

$$V_{far\_m} = V - mV_{near} \quad (3)$$

where  $C_{near\_m}(t)$  and  $C_{far\_m}(t)$  (plaque-forming unit [PFU]/m<sup>3</sup>) are the concentrations of virus in the near-field and far-field, respectively, in the train car when  $m$  infected persons (i.e. infectors) are present;  $E$  (PFU/h) is the rate of virus emission from an infector;  $F$  (m<sup>3</sup>/h) is the air flow volume rate from the near-field to the far-field and from near-field to far-field;  $I$  (m<sup>3</sup>/h) is the inhalation rate of a commuter;  $d_{inhalation}$  (unitless) is the deposition fraction in alveoli, conducting airways, and head airways;  $\lambda$ ,  $N$ , and  $d$  (/h) are the inactivation rate, air exchange rate, and deposition rate on indoor surfaces, respectively;  $V_{near}$ ,  $V_{far\_m}$ , and  $V$  (m<sup>3</sup>) are the estimated near-field volumes, far-field volumes, and total indoor volume of the train car; and  $n_{near}$  and  $n_{far\_m}$  (unitless) are the expected number of commuters in a near-field and a far-field, respectively. The near-field was set as an ellipsoid (minor radius, 0.25 m; major radius, 0.5 m) in front of the infector. The expected numbers of commuters in the near-field and far-field ( $n_{near}$  and  $n_{far\_m}$ ) were assigned according to the ratio of the projected area of the near-field to the floor and the rest area of the floor. The air completely mixed in the near-field was assumed to exchange with the air completely mixed in the far-field through half of the surface area of the ellipsoid according to the indoor air flow velocity (Spencer and Plisko 2007). The in-car air flow velocity with the AC/fan off during the stationary test was substituted for the in-car air flow velocity with the AC/fan on while the train was moving because the in-car air flow velocity with the AC/fan on did not differ between stationary and moving tests (Fig. S6). The number of viruses in the droplet nuclei generated during breathing and talking was assumed to be equal to that in the original droplets, wherein the virus concentration is assumed to be equal to that in the saliva.

The infection risk for a commuter in the near-field and far-field when  $m$  infectors are in the train car,  $R_{near\_m}$  and  $R_{far\_m}$  (unitless), respectively, can be expressed through the following equation, which is based on the general exponential model (Nicas and Jones, 2009; Watanabe et al., 2010; Haas et al., 2014):

$$R_{near\_m} = 1 - \exp(-kI \int_0^{t_c} C_{near\_m}(t) dt) \quad (4)$$

$$R_{far\_m} = 1 - \exp(-kI \int_0^{t_c} C_{far\_m}(t) dt) \quad (5)$$

where  $k$  (/PFU) is the dose–response function for SARS-CoV-2,  $I$  (m<sup>3</sup>/h) is the inhalation rate of a passenger,  $t_c$  (h) is the commute time of the infector, and  $C_{near\_m}(t)$  and  $C_{far\_m}(t)$  (PFU/m<sup>3</sup>) are the estimated exposure concentrations of the virus in the near-field and far-field when  $m$  infectors are present.

When we consider the community infection rate, the infection risk in the train car,  $R_{train}$ , can be expressed by using a binomial distribution as:

$$R_{train} = \sum_{m=1}^i n C_m r^m (1-r)^{n-m} \left( R_{near\_m} \frac{m n_{near}}{n} + R_{far\_m} \frac{n_{far\_m}}{n} \right) (i \leq n-1) \quad (6)$$

where  $i$  (unitless) is the maximum number of infected individuals on the train ( $m$ ),  $r$  (unitless) is the community infection rate, and  $n$  (unitless) is the total number of commuters in the entire train ( $n = m n_{near} + n_{far\_m}$ ). Because there is little additional contribution from  $i$  when  $i > 5$ , the calculation was approximated using  $i \leq 5$ .

The parameters and parameter derivation methods are listed in Table 1.

### 3. Results

Because of the public need for a rapid report, the air exchange rate data from the August 2020 survey are available in part on the website of the National Institute of Advanced Industrial Science and Technology (AIST, 2020).

#### 3.1. Stationary tests

Representative CO<sub>2</sub> concentration decay profiles are shown in Fig. S3. In the stationary tests, the air exchange rates in a car with all doors closed increased as the open area of windows increased (from 0.60/h with all windows closed to 4.4/h with all windows fully open in July, 0.59–0.78 to 9.9/h in August, and from 0.32 to 0.46/h to 4.0/h in December with the AC/fan on, and from 0.23/h to 2.1/h in July, 0.59 to 10/h in August, and from 0.48 to 0.54/h to 3.6–4.4/h in December with the AC/fan off; Fig. 2). At similar window-opening areas, air exchange rates were similar for in all cases of paired diagonal windows, 6 windows, and all 12 windows open (Fig. 2).

Average air exchange rates were higher when the AC/fan was on than when it was off during the July test (Fig. 2). The variation in the air exchange rates (mean  $\pm$  SD) among positions in the car was lower when the AC/fan was on ( $5.5\% \pm 4.4\%$  in July,  $3.2\% \pm 0.99\%$  in August, and  $7.2\% \pm 4.2\%$  in December) than when it was off ( $20\% \pm 8.7\%$  in July,  $25\% \pm 17\%$  in August, and  $11\% \pm 5.8\%$  in December).

In the stationary tests, air exchange rates were positively correlated with the absolute value of the indoor–outdoor temperature difference (Fig. S4). However, they were more strongly correlated with the window-opening area (Fig. 2). Air exchange rates were similar whether the 230 mannequins were present or not (Fig. S5).

In the doors-open condition, air exchange rates were similar regardless of the size of the window opening (Fig. 3). The air exchange rates with the doors open were lower when the AC/fan was on (averages of 12/h in July, 38/h in August, and 29/h in December with the heater off) than when it was off (averages of 30/h in July, 58/h in August, and 62/h in December with the heater off, and 70/h in December with the heater on).

#### 3.2. Moving test

The air exchange rates in the car with all 12 windows open to 10 cm increased as the train speed increased, from 10/h at 20 km/h to 42/h at 57 km/h (Fig. 4). Aboveground air exchange rates with all 12 windows open to 10 cm were approximately half the underground rates (Fig. 4). Aboveground air exchange rates when windows were closed were 3.1/h. In moving trains with all windows open, aboveground air exchange rates were similar regardless of the presence or absence of mannequins (Fig. 4).

#### 3.3. Air flow velocity and airtightness

During stationary tests with doors closed, the air flow velocity was similar regardless of the window-opening area. Air flow velocities were higher when the AC/fan was on (average, 0.21 m/s) than when it was off (average, 0.0088 m/s; Fig. S5). They were higher when doors were open (0.38 and 0.034 m/s for AC/fan on and off, respectively), but did not related to the window-opening area (Fig. S6). When the train was moving, air flow velocities with the AC/fan on were 0.19–0.31 m/s and did not differ with train speed (Fig. S6). The total leakage area of the car was 299 cm<sup>2</sup> and the C-value (gap area per floor area) was 5.4 cm<sup>2</sup>/m<sup>2</sup>.

#### 3.4. Evaluation of airborne infection risk

Estimated virus concentrations in the car are shown in Figures S7 and S8. Representative estimated risks of COVID-19 infection in the near-field and far-field are shown in Fig. S9. The infection risk of a passenger within 50 cm in front of a talking infected person when a single infected person is in the car ( $R_{near\_1}$ ) carrying 150 passengers travelling for 30 min in the context of a community infection rate of 0.30% is  $8.5 \times 10^{-5}$  with the windows closed and AC/fan off, however dropped to  $5.0 \times 10^{-6}$  with the window open and AC/fan on.

The estimated infection risks in a train car ( $R_{train}$ ), carrying 150 passengers for 30 min at a community infection rate of 0.30%, with

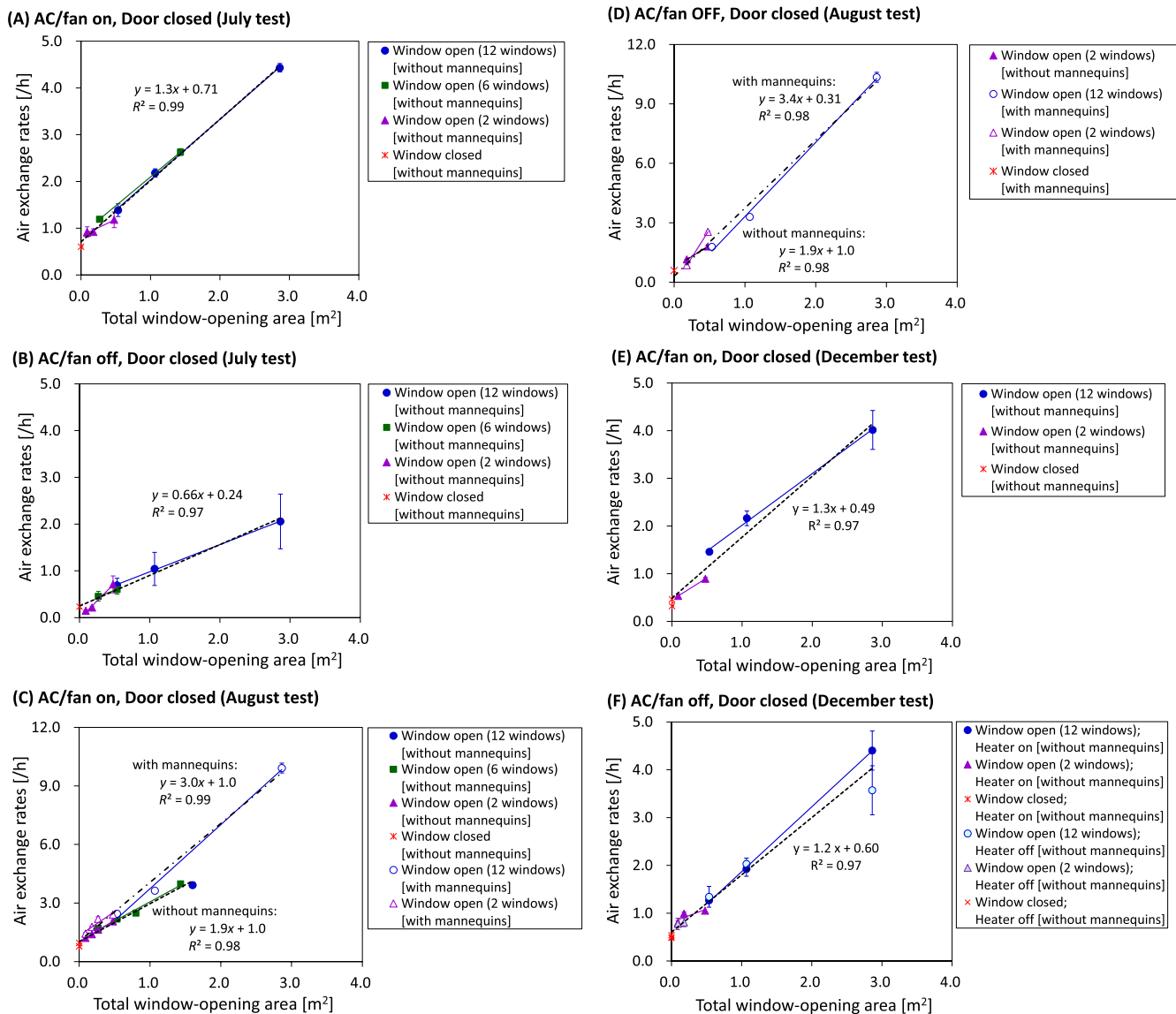


Fig. 2. Relationships between window-opening area and air exchange rates when doors were closed. (A) AC/fan on, July 2020, (B) AC/fan off, July 2020, (C) AC/fan on, August 2020, (D) AC/fan on, December 2020, (E) AC/fan off, December 2020. The regression lines were drawn by using all data from all window-opening positions. Error bars show the SD of the air exchange rates obtained from all 21 sampling points.

closed window and AC/fan off were reduced from  $2.5 \times 10^{-8}$  when the infected persons were silent and  $1.5 \times 10^{-7}$  when the infected persons were talking to  $1.7 \times 10^{-9}$  and  $1.1 \times 10^{-8}$ , respectively, when all 12 windows were open to 10 cm and the AC/fan was on (Figs. 5 and 6; Table S1). Assuming that 30–300 passengers traveled on trains for 7–60 min in the context of a community infection rate of 0.0050–0.30%, the risk of airborne infection risk in a train car ( $R_{train}$ ) was estimated to be reduced by 91–94% when windows were open (12 windows each open to 10 cm) and the AC/fan was on compared with when windows were shut and the AC/fan was off (Table S1).

#### 4. Discussion

Despite their importance for deriving countermeasures to COVID-19, air exchange rates in commuter trains have not been reported to date. We found that the air exchange rates in stationary train cars were strongly correlated with the window-opening area. In residential houses, the duration and degree of window-opening were strongly associated with air exchange rates (Shinohara et al., 2011; Hou et al., 2018). CFD calculations and wind tunnel experiments demonstrated that air

exchange rates were related to the window-opening area (Larsen and Heiselberg, 2008). In buildings, the natural ventilation volume is well known to be correlated with the window-opening area (Kurabuchi, 2016). Therefore, the natural ventilation of trains can be considered similar to that of buildings. In the present study, the stationary tests were conducted in the depot, with its shutters, doors, and windows closed, so the effect of wind outside the train was negligible. Previous CFD calculations and wind tunnel experiments have indicated that air exchange rates increase when the wind speed is high, especially when the wind direction is perpendicular to the windows (Gratia et al., 2004; Larsen and Heiselberg, 2008). Therefore, the air exchange rates we obtained may increase if strong crosswind is blow in a real station environment.

The air exchange rates in train cars were correlated with the indoor–outdoor temperature difference. Previous CFD calculations and wind tunnel experiments demonstrated that the air exchange rates varied depending on indoor–outdoor temperature differences when the wind direction was parallel to windows or the wind speed was null (Gratia et al., 2004; Larsen and Heiselberg, 2008). In addition, the relative effect of the temperature difference on air exchange rates

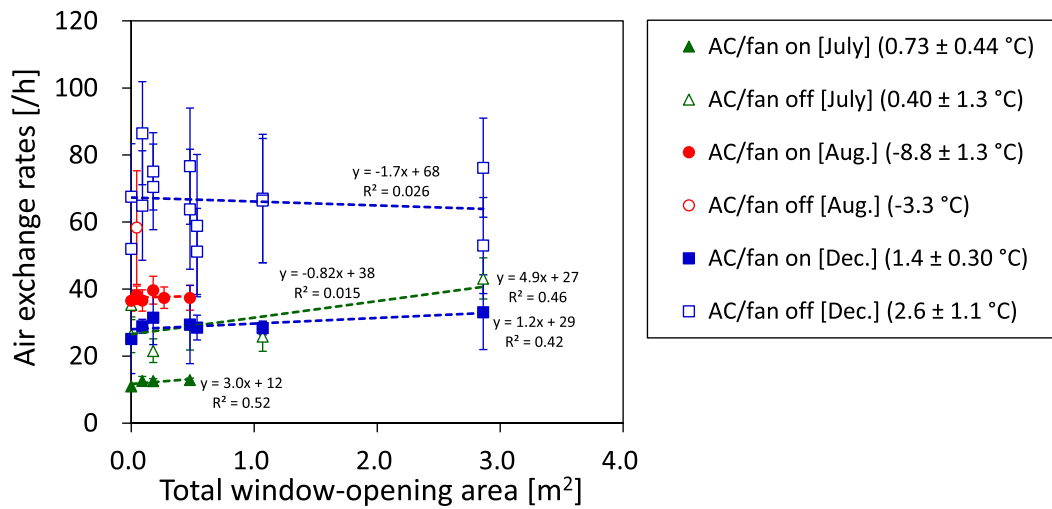


**Fig. 3.** Relationship between air exchange rates and window-opening area when doors were open. Error bars show SD of the air exchange rates obtained from all 21 sampling points.

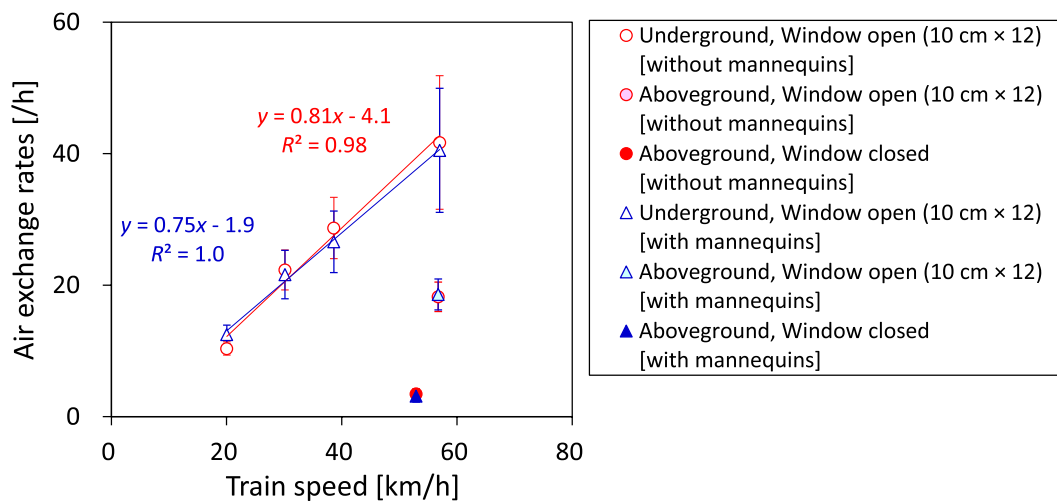


**Fig. 4.** Relationships between air exchange rates and train speed when all doors were closed. Error bars show SD of the air exchange rates obtained from all 21 sampling points.

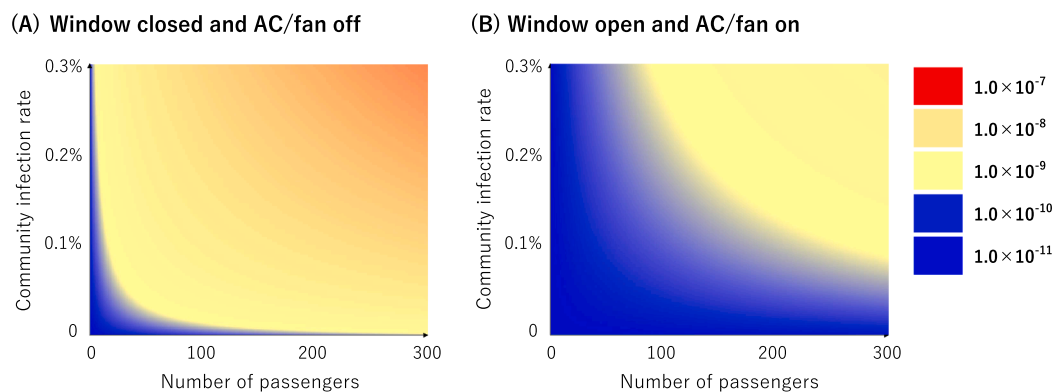


**Fig. 5.** Risk of COVID-19 infection in a train car,  $R_{\text{train}}$ , according to the community infection rate and number of passengers during a 30 min commute, assuming that infected persons were silent during the trip. (A) AC/fan off, windows closed. (B) AC/fan on, windows open.

decreased when the outdoor wind speed increased (Larsen and Heiselberg, 2008). Our study was conducted in a closed train depot in still air, and the obtained air exchange rates were related to the indoor-outdoor temperature difference.

In the December survey, the air exchange rates remained similar regardless of whether the heater was on or off. In the survey, temperature differences were similar between the heater-on and heater-off conditions probably because of the short test interval and the

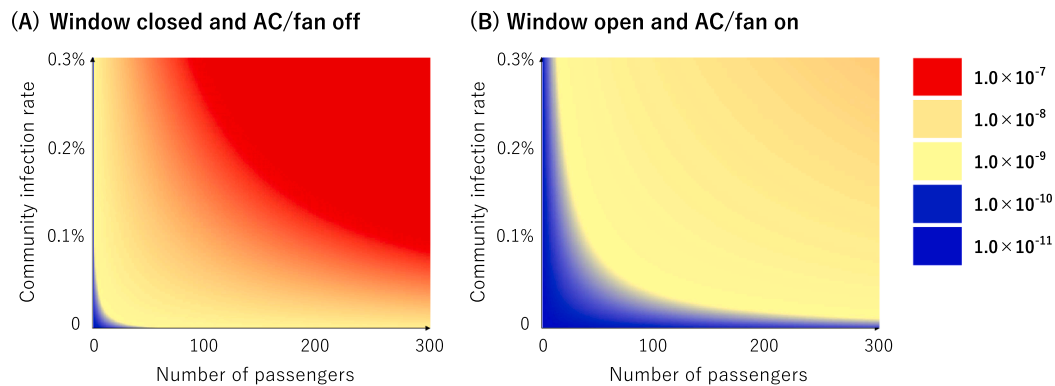


**Fig. 6.** Risk of COVID-19 infection in a train car,  $R_{train}$ , according to the community infection rate and number of passengers during a 30 min commute, assuming that infected persons were talking during the trip. (A) AC/fan off, windows closed. (B) AC/fan on and windows open.

relatively high in-car temperature even with the heater off. Under real-world conditions, the temperature differences and thus air exchange rates might decrease when the heater is off.

The air exchange rates with the doors closed were higher with the AC/fan on than off. Air exchange rates in buildings are increased when the outdoor wind speed is high (Gratia et al., 2004; Larsen and Heiselberg, 2008). The air exchange rates may depend on in-car air-flow velocity; indeed, they were substantially higher when the AC/fan was on than when it was off. By contrast, air exchange rates when the doors were open were higher with the AC/fan off, perhaps because of non-uniformity of in-car under these conditions.

During tests while the train was moving, the air exchange rates depended on the train speed, which may exert the same effects as those of wind speed. Furthermore, the air exchange rates were lower when the train was running aboveground rather than underground. This result might reflect differences in the indoor–outdoor air pressure, which were larger underground than aboveground (data not shown).

When air exchange rates were equal, the air exchange volume in the train car with mannequins was 11% lower than that without mannequins owing to the volume of the mannequins ( $12 \text{ m}^3$ ) relative to that of an empty car ( $107 \text{ m}^3$ ). In addition, the air exchange volume might decrease further in the presence of passengers owing to inhibition of air flow. The decrease in the air exchange volume in the train with 230 mannequins was observed to be only 15% compared to that without mannequins in the present study. It indicated that the presence of the mannequins did not significantly affect the air exchange volume. However, the upward current due to the heat generated by passengers, transfer of air caused by passenger flow, and air disturbance caused by passengers talking and breathing might all affect air exchange rates. Therefore, these effects should be elucidated in future studies.

The C-value of the train cars ( $5.4 \text{ cm}^2/\text{m}^2$ ) was much higher than that measured in residential houses ( $0.16\text{--}0.63 \text{ cm}^2/\text{m}^2$ ; Ikehara and Sakai, 2018). From both functional and structural viewpoints, the interior of the train car had many gaps. The total leakage area of the car determined in the airtightness test ( $0.029 \text{ m}^2$ ) was smaller than that assumed from the intercept of the regression line of the air exchange rates and window-opening area (approximately  $2 \text{ m}^2$ ). One possible cause of this difference is that the airtightness test directly determines the serial composition of the inlet and outlet gap areas, whereas the inlet gap areas might be calculated from measurements of the air exchange rates. The gaps in the inside walls of train car, which is more likely to influence air exchange rates, were much larger than the gaps in the outside wall, which is associated with airtightness. Another cause might be the inaccuracy in the airtightness test, which revealed small differences in air pressure between inside and outside of the car in the present study.

Because we used a passive  $\text{CO}_2$  monitor, rather than active monitor that aspirated air by pump, there was a delay in the response time. Therefore, larger air exchange rates may be underestimated. However,

there was no reversal of the large and small relationship of the air exchange rates.

When considering the same dose of virus, airborne routes may be more infective than other routes, because droplet nuclei can directly reach conducting airways and alveoli. Mizukoshi et al. (2021) estimated the airborne infection risk for cases wherein the dose–response function,  $k$ , was increased by 100. Here, when we increased  $k$  by a factor of 100 to 0.246, the risk of infection increased by almost 100-fold over the original value. Furthermore, some variant SARS-CoV-2 viruses might be much more infective. If infectivity is increased by 100-fold because of a virus variant, the infection risk increases by approximately 100-fold. Our findings suggest that window-opening and running the AC/fan might reduce the airborne infection risk in trains by 91–94%, an approximately comparable amount.

The airborne infection risk of COVID-19 in the context of a 0.30% community infection rate was estimated to be  $1.5 \times 10^{-7}$  when infected persons talked during a 30 min ride in a crowded train (150 commuters), even with the windows closed and the AC/fan off. In other words, given 8.4 million daily train-based commuters in Tokyo (MLIT, 2017), 1.3 commuters would become infected each day on trains when 3000 persons newly infected each day in Tokyo. It should be noted, however, that the estimated absolute number of infected people can be as much as 100-fold uncertain, as mentioned above. Recent case-control research has indicated that the use of public transport—unlike dining in restaurants and going to bars or coffee shops—did not increase the risk of COVID-19 infection (Mark et al. 2021).

To gauge the uncertainty in the assumed volume of the near-field, when we calculated the risk by 10-fold increase the volume with the same shape (major radius increased from 0.50 m to 1.1 m), the infection risk of a passenger in near-field ( $R_{near,1}$ ) decreased by 93% ( $5.9 \times 10^{-6}$ ) with the windows closed and the AC/fan off and by 92% ( $4.2 \times 10^{-7}$ ) with windows open and the AC/fan on. These results indicate that the airborne infection risk is greatly decreased from 50 cm in front of an infected person to 1.1 m. At this increased volume of near-field, the airborne infection risk in a train car ( $R_{train}$ ) decreased by 93% for windows closed and the AC/fan off and by 89–91% with windows open and the AC/fan on. To gauge the uncertainty in the assumed air flow volume rate from near-field to far-field, we calculated the risk associated with a 3-fold increase and one-third reduction in air flow volume. Consequently, the airborne infection risk in a train car ( $R_{train}$ ) decreased by 62–65% and increased by 2.6- to 2.9-fold, respectively, when windows were closed and the AC/fan was off and decreased by 48–63% and increased 2.1- to 2.5-fold, respectively, when the windows open and the AC/fan was on. The risk reduction associated with open windows and the AC/fan on did not differ markedly (0.89–6.4%) under these theoretical changes in air flow.

We did not estimate the droplet infection risk because most commuters in Japan currently wear masks and avoid speaking loudly on

trains. The risk might increase when some passengers talk loudly or do not wear masks. In addition, although viral copies were not detected at high concentrations on surfaces even in rooms inhabited by infected persons, and even though viable viruses were detected only rarely (Yamagishi et al., 2020), contact-based transmission by SARS-CoV-2 while commuting by train may not be ruled out. Estimating the risks associated with these transmission routes should be the subject of future research. Furthermore, opening the windows on moving train presents concerns regarding the risk of exposure to outdoor pollutants, noise, summer heat, and winter cold and merits risk-tradeoff analysis.

One limitation of the risk evaluation in the present study is related to the dose–response curve. We used the dose–response curve for mice death with SARS-CoV as an alternative for human infection with SARS-CoV-2. Although the basic reproduction number ( $R_0$ ) of SARS-CoV-2 was similar to that of SARS-CoV (Mizukoshi et al., 2021), it would be preferable to estimate risk by using the dose–response curve for SARS-CoV-2 when it becomes available. Regardless, using a mouse death dose–response relationship as a surrogate for an unavailable infection human dose–response relationship is generally accepted in human infection risk studies (Haas et al., 2014; Mizukoshi et al., 2021).

## 5. Conclusion

During stationary tests, the air exchange rates in train cars were strongly correlated with the window-opening area and weakly correlated with indoor–outdoor temperature differences. When doors were closed, air exchange rates were higher when the AC/fan was on than when it was off. It was observed that the door-opening had a significant influence on increase in ventilation rates. During tests of moving trains, air exchange rates in cars were strongly correlated with the train speed. By opening windows and turning on the AC/fan, commuters' infection risk in trains may be reduced by 91–94%. A risk-tradeoff analysis with the window-opening—which decreases virus exposure but increases exposure to outdoor pollutants, noise, and heat or cold—is warranted. The effectiveness of air purifiers and AC filters as alternatives to window-opening should be evaluated as well.

## CRediT authorship contribution statement

**Naohide Shinohara:** Project administration, Conceptualization, Methodology, Investigation, Formal analysis, Validation, Visualization, Writing – original draft, Writing – review & editing. **Jun Sakaguchi:** Methodology, Investigation, Writing – review & editing. **Hoon Kim:** Methodology, Investigation, Writing – review & editing. **Naoki Kagi:** Methodology, Investigation, Writing – review & editing. **Koichi Tatsu:** Methodology, Writing – review & editing. **Hiroyuki Mano:** Investigation, Writing – review & editing. **Yuichi Iwasaki:** Investigation, Writing – review & editing. **Wataru Naito:** Conceptualization, Methodology, Investigation, Writing – review & editing.

## Declaration of Competing Interest

The authors declare that they have no known competing financial interests or personal relationships that could have appeared to influence the work reported in this paper.

## Acknowledgements

We would like to express our gratitude to Tokyo Metro Co., Ltd. for providing the measurement environment and Taiyokogei Co., Ltd. for providing the mannequins for this study. We would like to express our gratitude to Mr. Akihiro Nagao from Espec Co., Ltd., Mr. Yasuhiko Ota from Isuzu Advanced Engineering Center, Ltd., and Mr. Isao Uchiyama, Mr. Hoshino Kunihiro, Mr. Taizo Higashiyama, Mr. Keisuke Hayakawa, and Mr. Futoshi Yoshimura from Kanomax Japan, Inc., for the assistance in the survey.

## Appendix A. Supplementary material

Supplementary data to this article can be found online at <https://doi.org/10.1016/j.envint.2021.106774>.

## References

- AIST, 2020. Efficacy of ventilation in subway vehicle including window opening. In: New Research Results. National Institute of Advanced Industrial Science and Technology, Japan (in Japanese). [https://www.aist.go.jp/aist\\_j/new\\_research/2020/nr20201203/nr20201203.html](https://www.aist.go.jp/aist_j/new_research/2020/nr20201203/nr20201203.html).
- AIST, 2007. Inhalation rates. The Japanese Exposure Factors Handbook. National Institute of Advanced Industrial Science and Technology, Research Center for Chemical Risk Management, Ibaraki, Japan. [https://unit.aist.go.jp/riss/crm/exposurefactors/documents/factor/body/breathing\\_rate.pdf](https://unit.aist.go.jp/riss/crm/exposurefactors/documents/factor/body/breathing_rate.pdf) (accessed 31 January 2021).
- ASTM: America Society for Testing and Materials, 1998. ASTM D6245: Standard Guide for Using Indoor Carbon Dioxide Concentrations to Evaluate Indoor Air Quality and Ventilation.
- Asai, T., 1995. Numerical simulation on indoor air pollution and aerosol. *Eazozoru Kenkyu*, 10, 179–184 (in Japanese).
- Beko, G., Lund, T., Nors, F., Toftum, J., Clausen, G., 2010. Ventilation rates in the bedrooms of 500 Danish children. *Build. Environ.* 45, 2289–2295. <https://doi.org/10.1016/j.buildenv.2010.04.014>.
- Bourouiba, L., 2021. The fluid dynamics of disease transmission. *Annu. Rev. Fluid Mech.* 53, 473–508. <https://doi.org/10.1146/annurev-fluid-060220113712>.
- Buonanno, G., Stabile, L., Morawska, L., 2020. Estimation of airborne viral emission: Quanta emission rate of SARS-CoV-2 for infection risk assessment. *Environ. Int.* 141, 105794. <https://doi.org/10.1016/j.envint.2020.105794>.
- Chen, L.L., Ban, G.Z., Long, E.S., Kalonji, G., Cheng, Z., Zhang, L., Guo, S.R., in press. Estimation of the SARS-CoV-2 transmission probability in confined traffic space and evaluation of the mitigation strategies. *Environ. Sci. Pollut. Res.* <https://doi.org/10.1007/s11356-021-13617-y>.
- Dai, H., Zhao, B., 2020. Association of the infection probability of COVID-19 with ventilation rates in confined spaces. *Build. Simul.* 13, 1321–1327. <https://doi.org/10.1007/s12273-020-0703-5>.
- Gratia, E., Bruyere, I., De Herde, A., 2004. How to use natural ventilation to cool narrow office buildings. *Build. Environ.* 39, 1170–11157. <https://doi.org/10.1016/j.buildenv.2004.02.005>.
- Haas, C.N., Rose, J.B., Gerba, C.P., 2014. Quantitative microbial risk assessment, second ed. In: Haas, C.N., Rose, J.B., Gerba, C.P., (Eds.). Chapter 9 Uncertainty. Hoboken, NJ: John Wiley & Sons, Inc., pp. 323–376.
- Haas, C.N., 1983. Estimation of risk due to low doses of microorganisms: a comparison of alternative methodologies. *Am. J. Epidemiol.* 118, 573–582. <https://doi.org/10.1093/oxfordjournals.aje.a113662>.
- Harrichandra, A., Ierardi, A.M., Pavilonis, B., 2020. An estimation of airborne SARS-CoV-2 infection transmission risk in New York City nail salons. *Toxicol. Ind. Health* 36, 634–643. <https://doi.org/10.1177/0748233720964650>.
- Hou, J., Zhang, Y.F., Sun, Y.X., Wang, P., Zhang, Q.N., Kong, X.R., Sundell, J., 2018. Air change rates at night in northeast Chinese homes. *Building Environ.* 132, 273–281. <https://doi.org/10.1016/j.buildenv.2018.01.030>.
- Ikehara, M., Sakai, E., 2018. Study and Assessment on the Airtight Performance of Dwelling Units in Newly Built Apartment Buildings. In: Report on Engineering Research and Development (Sumitomo Mitsui Construction Co., LTD.), vol. 16, pp. 83–87 (in Japanese). <https://www.smcon.co.jp/service/assets/uploads/RandD/report-2018/r-11.pdf>.
- JISC, 1974. Japanese Industrial Standards Committee. JIS-1406: Method for Measuring Amount of Room Ventilation (Carbon Dioxide Method) [in Japanese]. <http://kikakurui.com/a1/A1406-1974-01.html>.
- JMA: Japan Meteorological Agency, 2021. Weather statistics. (JMA website; in Japanese). <http://www.data.jma.go.jp/obd/stats/etrn/index.php/> (accessed 10 May 2021).
- Jones, R.M., Brosseau, L.M., 2015. Aerosol transmission of infectious disease. *J. Occup. Environ. Med.* 57, 501–508. <https://doi.org/10.1097/JOM.0000000000000448>.
- Kurabuchi, T., 2016. Architecture Course for Beginners – Building Environment, third ed., Ichigaya Publishing Co., Ltd., Tokyo, Japan.
- Larsen, T.S., Heiselberg, P., 2008. Single-sided natural ventilation driven by wind pressure and temperature difference. *Energy Build.* 40, 1031–1040. <https://doi.org/10.1016/j.enbuild.2006.07.012>.
- Li, N., Yang, L., Li, X.D., Li, X.D., Tu, J.Y., Cheung, S.C.P., 2019. Multi-objective optimization for designing of high-speed train cabin ventilation system using particle swarm optimization and multi-fidelity Kriging. *Build. Environ.* 155, 161–174. <https://doi.org/10.1016/j.buildenv.2019.03.021>.
- Li, Y., Qian, H., Hang, J., Chen, X., Cheng, P., Ling, H., Wang, S., Liang, P., Li, J., Xiao, S., Wei, J., Liu, L., Cowling, B.J., Kang, M., 2021. Probable airborne transmission of SARS-CoV-2 in a poorly ventilated restaurant. *Build. Environ.* 196, 107788. <https://doi.org/10.1016/j.buildenv.2021.107788>.
- Mark, W.T., Kiva, A.F., Manish, M.P., 2021. Identifying COVID-19 risk through observational studies to inform control measures. *JAMA*. <https://doi.org/10.1001/jama.2021.1995>.
- MHLW: Ministry of Health, Labour and Welfare, 2021. Views on measures against COVID-19, Novel Coronavirus Expert Meeting. <https://www.mhlw.go.jp/content/1090000/00060606000.pdf> (accessed 31 January 2021).
- Miller, S.L., Nazaroff, W.W., Jimenez, J.L., Boerstra, A., Buonanno, G., Dancer, S.J., Kurnitski, J., Marr, L.C., Morawska, L., Noakes, C., 2020. Transmission of SARS-CoV-

- 2 by inhalation of respiratory aerosol in the Skagit Valley Chorale superspreading event. *Indoor Air* 31, 314–323. <https://doi.org/10.1111/ina.12751>.
- Mitchell, J., Weir, M., 2020. SARS: Dose response experiments. QMRA Wiki web sites. <http://qmrwiki.org/experiments/sars> (accessed 5 March 2021).
- Mizukoshi, A., Nakama, C., Okumura, J., Azuma, K., 2021. Assessing the risk of COVID-19 from multiple pathways of exposure to SARS-CoV-2: Modeling in health-care settings and effectiveness of nonpharmaceutical interventions. *Environ. Int.* 147, 106338. <https://doi.org/10.1016/j.envint.2020.106338>.
- MLIT, 2017. Metropolitan transportation census in Tokyo metropolitan area. Ministry of Land, Infrastructure, Transport and Tourism, Japan. <https://www.mlit.go.jp/common/001179760.pdf> (accessed 7 July 2021).
- MLIT, 2020. Congestion rates of major sections in Tokyo metropolitan area at 2019. Ministry of Land, Infrastructure, Transport and Tourism, Japan. <https://www.mlit.go.jp/report/press/content/001364124.pdf> (accessed 7 July 2021).
- Morawska, L., Johnson, G.R., Ristovski, Z.D., Hargreaves, M., Mengersen, K., Corbett, S., Chao, C.Y.H., Li, Y., Katoshevski, D., 2009. Size distribution and sites of origin of droplets expelled from the human respiratory tract during expiratory activities. *J. Aerosol Sci.* 40, 256–269. <https://doi.org/10.1016/j.jaerosci.2008.11.002>.
- Munster, V.J., Feldmann, F., Williamson, B.N., van Doremalen, N., Perez-Perez, L., Schulz, J., Meade-White, K., Okumura, A., Callison, J., Brumbaugh, B., Avanzato, V. A., Rosenke, R., Hanley, P.W., Saturday, G., Scott, D., Fischer, E.R., de Wit, E., 2020. Respiratory disease in rhesus macaques inoculated with SARS-CoV-2. *Nature* 585, 268–272. <https://doi.org/10.1038/s41586-020-2324-7>.
- Murakami, M., Miura, F., Kitajima, M., Fujii, K., Yasutaka, T., Iwasaki, Y., Ono, K., Shimazu, Y., Sorano, S., Okuda, T., Ozaki, A., Katayama, K., Nishikawa, Y., Kobashi, Y., Sawano, T., Abe, T., Saito, M., Tsubokura, M., Naito, W., Imoto, S., 2021. COVID-19 risk assessment at the opening ceremony of the Tokyo 2020 Olympic Games. *Microbial Risk Analysis* 21, 100162. <https://doi.org/10.1016/j.mran.2021.100162>.
- Nicas, M., Sun, G., 2006. An integrated model of infection risk in a health-care environment. *Risk Anal.* 26, 1085–1096. <https://doi.org/10.1111/j.1539-6924.2006.00802.x>.
- Nicas, M., Jones, R.M., 2009. Relative contributions of four exposure pathways to influenza infection risk. *Risk Anal.* 29, 1292–1303. <https://doi.org/10.1111/j.1539-6924.2009.01253.x>.
- Riley, E.C., Murphy, G., Riley, R.L., 1978. Airborne spread of measles in a suburban elementary school. *Am. J. Epidemiol.* 107, 421–432. <https://doi.org/10.1093/oxfordjournals.aje.a112560>.
- RIVM: National Institute for Public Health and the Environment, 2017. Multiple path particle dosimetry model (MPPD v.3.04): a model for human and rat airway particle dosimetry. RIVA Report 650010030. Bilthoven, Netherlands.
- Schijven, J., Vermeulen, L.C., Swart, A., Meijer, A., Duizer, E., Husman, A.M.D., 2020. Quantitative microbial risk assessment for airborne transmission of SARS-CoV-2 via breathing, speaking, singing, coughing, and sneezing. *Environ. Health Perspect.* 129, 047002. <https://doi.org/10.1289/EHP7886>.
- Shen, Y., Li, C.W., Dong, H.J., Wang, Z., Martinez, L., Sun, Z., Handel, A., Chen, Z.P., Chen, E.F., Ebell, M.H., Wang, F., Yi, B., Wang, H.B., Wang, X.X., Wang, A.H., Chen, B.B., Qi, Y.L., Liang, L.R., Li, Y., Ling, F., Chen, J.F., Xu, G.Z., 2020. Community outbreak investigation of SARS-CoV-2 transmission among bus riders in Eastern China. *JAMA Int. Med.* 180, 1665–1671. <https://doi.org/10.1001/jamainternmed.2020.5225>.
- Shinohara, N., Kataoka, K., Takamine, M., Gamo, M., 2011. Distribution and variability of the 24-h average air exchange rates and interzonal flow rates in 26 Japanese residences over 5 seasons. *Atmospheric Environ.* 45, 3548–3552. <https://doi.org/10.1016/j.atmosenv.2011.04.005>.
- Shinohara, N., Tokumura, M., Kazama, M., Yoshino, H., Ochiai, S., Mizukoshi, A., 2013. Indoor air quality, air exchange rates, and radioactivity in new built temporary houses following the Great East Japan Earthquake in Minamisoma, Fukushima. *Indoor Air* 23, 332–341. <https://doi.org/10.1111/ina.12029>.
- Spencer, J.W., Plisko, B.M.J., 2007. Evaluation of a mathematical model for estimating solvent exposure in the workplace. *J. Occup. Environ. Hygiene* 4, 253–259. <https://doi.org/10.1080/15459620701205253>.
- Tang, S., Mao, Y.X., Jones, R.M., Tan, Q.Y., Ji, J.S., Li, N., Shen, J., Lv, Y.B., Pan, L.J., Ding, P., Wang, X.C., Wang, Y.B., MacIntyre, C.R., Shi, X.M., 2020. Aerosol transmission of SARS-CoV-2? Evidence, prevention and control. *Environ. Int.* 144, 106039. <https://doi.org/10.1016/j.envint.2020.106039>.
- To, G.N.S., Chao, C.Y.H., 2010. Review and comparison between the Wells-Riley and dose-response approaches to risk assessment of infectious respiratory diseases. *Indoor Air* 20, 2–16. <https://doi.org/10.1111/j.1600-0668.2009.00621.x>.
- To, K.K.W., Tsang, O.T.Y., Yip, C.C.Y., Chan, K.H., Wu, T.C., Chan, J.M.C., Leung, W.S., Chik, T.S.H., Choi, C.Y.C., Kandamby, D.H., Lung, D.C., Tam, A.R., Poon, R.W.S., Fung, A.Y.F., Hung, I.F.N., Cheng, V.C.C., Chan, J.F.W., Yuen, K.Y., 2020a. Consistent detection of the 2019 novel coronavirus in saliva. *Clin. Infect. Dis.* 71, 841–843. <https://doi.org/10.1093/cid/ciaa149>.
- To, K.K.W., Tsang, O.T.Y., Leung, W.S., Tam, A.R., Wu, T.C., Lung, D.C., Yip, C.C.Y., Cai, J.P., Chan, J.M.C., Chik, T.S.H., Lau, D.P.L., Choi, C.Y.C., Chen, L.L., Chan, W. M., Chan, K.H., Ip, J.D., Ng, A.C.K., Poon, R.W.S., Luo, C.T., Cheng, V.C.C., Chan, J. F.W., Hung, I.F.N., Chen, Z.W., Chen, H.L., Yuen, K.Y., 2020b. Temporal profiles of viral load in posterior oropharyngeal saliva samples and serum antibody responses during SARS-CoV-2 infection: an observational cohort study. *Lancet Infect. Dis.* 20565574. [https://doi.org/10.1016/S1473-3099\(20\)30196-1](https://doi.org/10.1016/S1473-3099(20)30196-1).
- Tokyo Metro, Route/Station Information, 2021. <https://www.tokymetro.jp/station/> (accessed 7 July).
- Tokyo Metropolitan Government, 2019. 2-1 Changes in Population, 2. Population and Households. Tokyo Statistical Yearbook 2019. <https://www.toukei.metro.tokyo.lg.jp/tnenkan/2019/tm19q3e002.htm>. (accessed 7 July 2021).
- Tokyo Metropolitan Government, 2021. Change in positive cases by reported day. Updates on COVID-19 in Tokyo. COVID-19 Information Website. <https://stopcovid19.metro.tokyo.lg.jp/en> (accessed 7 July 2021).
- Tsubokura, M., 2021. Prediction and countermeasure of virus droplet infection in indoor environment. <https://www.r-cs.riken.jp/outreach/formedia/200824Tsubokura/> (in Japanese) (accessed 5 March 2021).
- Uhteg, K., Jarrett, J., Richards, M., Howard, C., Morehead, E., Geahr, M., Gluck, L., Hanlon, A., Ellis, B., Kaur, H., Simmer, P., Carroll, K.C., Mostafa, H.H., 2020. Comparing the analytical performance of three SARS-CoV-2 molecular diagnostic assays. *J. Clin. Virol.* 127, 104384. <https://doi.org/10.1016/j.jcv.2020.104384>.
- van Doremalen, N., Bushmaker, T., Morris, D.H., Holbrook, M.G., Gamble, A., Williamson, B.N., Tamin, A., Harcourt, J.L., Thornburg, N.J., Gerber, S.I., Lloyd-Smith, J.O., de Wit, E., Munster, V.J., 2020. Aerosol and surface stability of SARS-CoV-2 as compared with SARS-CoV-1. *New Eng. J. Med.* 382, 1564–1567. <https://doi.org/10.1056/NEJMc2004973>.
- Wang, H., Lin, M., Chen, Y., 2014. Performance evaluation of air distribution systems in three different China railway high-speed train cabins using numerical simulation. *Building Simulat.* 7, 629–638. <https://doi.org/10.1007/s12273-014-0168-5>.
- Watanabe, T., Bartrand, T.A., Weir, M.H., Omura, T., Haas, C.N., 2010. Development of a dose-response model for SARS coronavirus. *Risk Anal.* 30, 1129–1138.
- Wells, W.F., 1934. On airborne infection. Study II. Droplet and droplet nuclei. *Am. J. Hygiene* 20, 611–618. <https://doi.org/10.1093/oxfordjournals.aje.a118097>.
- WHO. Director-General's opening remarks at the media briefing on COVID-19 – March 11, 2020. World Health Organization, Geneva.
- WHO, 2021. Coronavirus Disease (COVID-19) Dashboard; World Health Organization, Geneva. <https://covid19.who.int/> (accessed 31 January 2021).
- Wölfel, R., Corman, V.M., Guggemos, W., Seilmaier, M., Zange, S., Muller, M.A., Niemeyer, D., Jones, T.C., Vollmar, P., Rothe, C., Hoelscher, M., Bleicker, T., Brunink, S., Schneider, J., Ehmann, R., Zwirgmaier, K., Drosten, C., Wendtner, C., 2020. Virological assessment of hospitalized patients with COVID-2019. *Nature* 581, 465–469. <https://doi.org/10.1038/s41586-020-2196-x>.
- Wyllie, A.L., Fournier, J., Casanovas-Massana, A., Campbell, M., Tokuyama, M., Vijayakumar, P., Geng, B., Muenker, M.C., Moore, A.J., Vogels, C.B.F., Petrone, M.E., Ott, I.M., Lu, P., Venkataraman, A., Lu-Culligan, A., Klein, J., Earnest, R., Simonov, M., Datta, R., Handoko, R., Naushad, N., Sewanan, L.R., Valdez, J., White, E.B., Lapidus, S., Kalinich, C.C., Jiang, X., Kim, D.J., Kudo, E., Linehan, M., Mao, T., Moriyama, M., Oh, J.E., Park, A., Silva, J., Song, E., Takahashi, T., Taura, M., Weizman, O.-L., Wong, P., Yang, Y., Bermejo, S., Odio, C., Omer, S.B., Cruz, C.S.D., Farhadian, S., Martinello, R.A., Iwasaki, A., Grubaugh, N.D., Ko, A.I., 2020. Saliva or nasopharyngeal swab specimens for the detection of SARS-CoV-2. *N. Engl. J. Med.* 383, 1283–1286. <https://doi.org/10.1056/NEJMc2016359>.
- Xie, X., Li, Y., Chwan, A.T.Y., Ho, P.L., Seto, W.H., 2007. How far droplets can move in indoor environments – revisiting the Wells evaporation–falling curve. *Indoor Air* 17, 211–225. <https://doi.org/10.1111/j.1600-0668.2007.00469.x>.
- Yamagishi, T., Ohnishi, M., Matsunaga, N., Kakimoto, K., Kamiya, H., Okamoto, K., Suzuki, M., Gu, Y., Sakaguchi, M., Tajima, T., Takaya, S., Ohmagari, N., Takeda, M., Matsuyama, S., Shirato, K., Nao, N., Hasegawa, H., Kageyama, T., Takayama, I., Saito, S., Wada, K., Fujita, R., Saito, H., Okinaka, K., Griffith, M., Parry, A.E., Barnetson, B., Leonard, J., Wakita, T., 2020. Environmental sampling for severe acute respiratory syndrome coronavirus 2 during a COVID-19 outbreak on the diamond princess cruise ship. *J. Infect. Dis.* 222, 1098–1102. <https://doi.org/10.1093/infdis/jiaa437>.
- Yang, W., Marr, L.C., 2011. Dynamics of airborne influenza A viruses indoors and dependence on humidity. *PLoS ONE* 6, e21481. <https://doi.org/10.1371/journal.pone.0021481>.
- Zhu, N., Zhang, D., Wang, W., Li, X., Yang, B., Song, J., Zhao, X., Huang, B., Shi, W., Lu, R., Niu, P., Zhan, F., Ma, X., Wang, D., Xu, W., Wu, G., Gao, G.F., Tan, W.A., 2020. A novel coronavirus from patients with pneumonia in China, 2019. *N. Engl. J. Med.* 382, 727–733. <https://doi.org/10.1056/NEJMoa2001017>.